ANALYSIS AND PREDICTION OF FATIGUE CRACK PROPAGATION IN MACHINE AND PLANT COMPONENTS

H. FÖHRING*, V. KÖTTGEN** AND T. SEEGER**

An overview is given on fracture mechanics application in industry. Highlighted are crack propagation aspects of nuclear as well as aircraft engineering. Experimentally observed phenomena are correlated to fatigue fracture mechanics predictions. The role of constant amplitude crack growth functions as the basis of any more detailed crack life estimation by cycle-by-cycle prediction models is pointed out in addition to a discussion of two of the most actual models.

Fracture mechanics has numerous very different faces. Fig. 1 tries to give a tabulated overview on the field of machine and plant components where fracture mechanics is used in industry. Three main columns are related to Power Generation, Heavy Industry and Transport Vehicles and each is subdivided into three columns which are more specific.

The content of the first line "components" illustrates the variety of components and at the same time the impossibility to cover more than one or two industrial fields concerning fracture mechanics. The following lines "type of loading" and "materials" are filled mainly with keywords valid for all three subdivisions in each main column. Additionally, you find hints for special features, e.g. load history problems (waves, gust loads), relevant to our topic. The information on fracture mechanics application is subdivided into the sections "interests" and "problem areas" to correlate application to the different evolutionary stages of the components and to specific fracture mechanics disciplines, as well.

In Fig. 2 the content of the last two lines of Fig. 1 is brought into a somewhat artificial "order of rank". The intention behind is to point out the degree of penetration of fracture mechanics into the different industries. The two outermost bars of the figure are the highest ones which shall demonstrate that fracture mechanics is mostly used with the high performance structures of airplanes, space vehicles as well as nuclear power plants components but, as shown later, in a very different manner. In these fields, fracture mechanics is about to grow from the stage of "research and development" to the stage of "engineering application" which means the application of rules and codes with fracture mechanics background. Off-shore heavy industry is supposed to be the third in the club of "engineering application of fracture mechanics".

According to the title of the paper the authors treat fatigue problems only. The combination of the words "fatigue" and "fracture mechanics"

---

* Lahmeyer International, Consulting Engineers, Frankfurt F.R.G.

** Technical University of Darmstadt, Darmstadt F.R.G.

means crack growth under repeated loading. All load sequences represent nothing but idealizations of measured load histories. How to derive the representative load sequence from the measured load history is the field of counting methods, being a field of its own which is not to be treated in this paper. No question, each crack growth prediction needs its load history. As examples, Fig. 3 presents eight LBF-measurements: stress/pressure/bending moment/acceleration over time (various scales) from cars, (Number 1, 3, 5), airplanes (6, 8), a roll stand (4), an oil pipeline (7) and a condensation chamber of a boiling water reactor (2).

FRACTURE MECHANICS APPLIED TO NUCLEAR PIPING

As to the design concept the nuclear power industry on the one hand and the military aircraft industry on the other hand are the most extreme representatives. This is due to the very different safety requirements of the structural components influencing design details, manufacturing, construction, quality control and in-service inspection. Through that, it is necessary to know the whole concept when interpreting fracture mechanics solutions of the industry.

The pressure-retaining pipes of the primary circuit of a pressurized water reactor of the modern German reactor line follow the rules of the so-called "basic safety design". Those pipes are characterized by low primary stresses, thick walls, few welds, high alloy ferritic steel, highly detailed quality assurance with production and assembling in the plant as well as during service.

Fig. 4 represents the propagation curve of a circumferential crack in the main coolant piping, Bartholome et al. (1). The curve consists of two parts. The first curve commencing at the beginning of plant service describes the radial extension of the initial half-elliptical outer surface crack through the wall thickness. The second curve commences when the crack is broken through the wall thickness and extends circumferentially until final fracture. Three features are of interest:

First, life is estimated at the most critical pipe section applying all service loading cases including even postulated accidental events. Second, the time for the crack to grow through the wall thickness is more than ten times longer than rest of life till fracture. Third, look at the safety margin: the time axis is not on a year's scale but on a reactor life's scale. 50 reactor lives mean 50x40=2000 years!

Another example of nuclear piping follows, concerning the primary sodium piping system of the German fast breeder reactor SNR-300. The question to answer is: what is the safety margin in the case that leakage is only detectable when the leakage area has reached a magnitude of 1 mm^2?

This study is made for an axial through-crack in the hot leg (T=550°C) where creep crack growth prevails as well as in the cold leg (T=380°C) where fatigue crack growth prevails.

Fig. 5 shows a set of four curves: the leakage area grows with the growing crack (from left to right); the restlife diminishes with the growing crack. One pair of calculative curves holds for both the hot and the cold leg. The curves for the leakage area are very similar, whereas the restlife curves behave differently. Furtheron, the critical crack length of the hot leg amounts to approx. one half of that of the cold leg.

The answer to the question can be read from the diagram: a crack detected by leakage in the hot leg is correlated to approx. 500 days of continuous plant service, whereas a crack detected in the cold leg is correlated to approx. 7600 start-up/shut-down cycles.

This investigation undertaken under worst assumptions yielded that a through-crack whereever it might occur and whenever it will appear will be detected early enough to safely shut the reactor down for inspection.

CRACK TIP DAMAGE PHENOMENA IN THE VIEW OF FATIGUE FRACTURE MECHANICS

Eight years ago Führing and Seeger (2) created the term "fatigue fracture mechanics" for applying nonlinear fracture mechanics to crack growth under repeated loading including crack closure effects. They performed parametrical analyses that furnished deep insights into fatigue damage phenomena at crack tips.

When putting the special glasses of fatigue crack growth aside you notice, however, that very similar mechanisms occur at the crack tip in case of monotonic crack growth, too. As an example Fig. 6 shows a well-known picture of the load displacement diagram of a fracture mechanics specimen and the typical crack tip configurations that can be associated to the diagram. The extended Dugdale or strip yield model (3), (16) which was used for the Fatigue Fracture Mechanics calculations, actually is able to describe not only the blunting effect but also the tearing effect that is associated to the onset of rapid crack extension. The steps in the tearing crack profile Fig. 6d represent the hump of residual plastic displacements. That is the difference in crack profile between a stationary crack and a non-stationary crack of same length and maximum load. The observed crack opening displacement at the tip of an open crack, called CTOD, was originally supposed by Rice (4) to represent the strain of the unbroken volume element at the ligament ahead of the crack tip. This applies only in case of stationary cracks (mathematical saw cuts). However, this does not apply for non-stationary cracks, i.e. all cases where the crack has previously grown by fatigue or tearing, see the theoretical and experimental results presented in Figs. 7, 8.

As a consequence one cannot conclude from a measure of the crack opening profile in a straighforward way to the strain of the unbroken volume element although this is the only one where one can get in idea about the fracture process.

As to the crack profile, a difference between tearing under monotonic loading and repeated loading (fatigue crack growth) of constant amplitude (CA) must be pointed out. It concerns the magnitude of residual displacements at the wakes of the crack. The residual displacements along a fatigue crack where the half-length a is measured from x-origin are given by the expression (2)

$$v_{re}(x) = v_a(a=x) \neq \text{const.}$$

On the other hand, the residual displacements of the tearing crack of same definition are given by the expression, Seeger (5),

$$v_{re}(x) = v_{rupture} = \text{const.}$$

Possibly, the crack tip opening angle CTOA is a better material parameter than CTOD. According to (6) one gets the general CTOA expression for

the non-stationary crack as:

$$CTOA = 2\,[dv/dx + dv_{re}/dx]_{x=a}$$

In case of a fatigue crack at small scale yielding conditions according to the above-written expression it follows

$$CTOA = 2\,(2\frac{v_a}{\omega} + \frac{v_a}{a}) \qquad \text{(for CA loading)}$$

In the tearing case, the second term in brackets becomes zero, hence CTOA is smaller than for fatigue:

$$CTOA = 4\,v_a/\omega \qquad \text{(for monotonic loading)}$$

It should be emphasized that the expressions for the CTOD ($=2v_a$) of the crack tip element and the plastic zone size ω are the traditional ones which can be taken from (4) or similar references. These quantities are not subject to the kind of crack development either by CA or monotonic loading.

The experimentally observed craze zone and crack profile of a PMMA specimen, depicted in Fig. 7a, confirms the capability of the extended Dugdale model to realistically describe the fracture process. Compare the very similar displacement curves in the lower part of Fig. 7b. The distance between the crosses and the lines represents the measure of the residual displacements as predicted by the model. The model is not only supported by the mentioned displacement measurements but also by X-ray measurements of the residual stresses around the crack tip, e.g. Kunz et al. (8).

With reference (9) a strip yield solution to the contact problem is given by Budiansky and Hutchinson for the first time in a closed form. Because of two simplifying assumptions concerning the residual displacements and the contact stresses, the U(R) results of this publication are not recommended for use with crack growth estimations. The strong dependence of the U(R)-curve on the assumptions of the closure analysis has already been pointed out in reference (3).

As generally known, the U(R)-curve, i.e. the dependence of the effective stress ration U on the full stress ratio R, is the key to several modern crack growth prediction techniques. They will be described in the next sections of the paper.

The effective stress ratio as defined by Elber (15)

$$U = \frac{S_{max} - S_{op}}{S_{max} - S_{min}}$$

is based on the crack opening load S_{op} mostly evaluated from load-displacement curves of crack growth tests of the material and constant amplitude concerned. Experiences with the evaluation techniques for S_{op} are controversially discussed in many publications of the past years. Because of this unclear situation the present authors take the opportunity to comment on some typical observations. Since crack opening loads can be the result of very different measurement procedures (measurement technique and location of the measurement along the crack axis) the magnitude of the observed crack opening load (called S_{op}) can vary. Fig. 8 shows two

examples from Jones et al. (10) and Ohta et al. (11) where the "gage location" (the measuring point) obviously influences S_{op} in a certain way *. However, when measuring the bulk displacement behaviour of the specimen at locations away from the crack tip one does not get a physically reliable characterization of the crack tip. As already stated in connection with the CTOD measurements, only the answer of the material element just ahead of the crack is relevant for describing the fracture process nearest to the crack tip where the "real" crack opening level can be read of. All the other measurements are more or less insensitive, see references (3) and (13). To summarize in one sentence: the observed S_{op}-value becoming independent of the gage location means nothing else but that the measurement becomes insensitive with respect to the crack opening load.

According to the above statements, in Fig. 8 the real values are indicated by the arrows:

$S_{op}/S_{max} \simeq 0.65$ for $R = 0.1$ and

$U \simeq 0.15$ for $R = -1.0$

No question, real S_{op}-values are difficult to find. We are still away from being able to formulate generally applicable rules for the S_{op}-evaluation.

With Fig. 9 it is intended to focus on another independent verification of the extended Dugdale model. The model predicts that the cracked volume is stiffer during loading than during unloading of CA-cycling. The experiments by Sharpe and Grandt (12) reveal the same behaviour: when considering indentical load levels the crack is observed to be less open during loading than during unloading. This fact confirms former theoretical findings that the load needed to totally open the crack must be higher than the load where the crack wakes commence contact. Hence, for CA loading (13):

$$S_{opening} > S_{closure}$$

Because of conflicting experimental results this question, too, is under permanent discussion. As in the case mentioned before the controversy is supposed to be due to the use of insensitive measurement techniques or false interpretation of experimental results.

CONSTANT-AMPLITUDE CRACK GROWTH FUNCTIONS - BASIS OF PREDICTION METHODS

Typically, modelling for crack propagation prediction can be separated into two steps. In the first step some sort of "effective" interior loading is determined as a fraction of the applied exterior loading. In the second step an actual increment of crack growth is deduced from the "effective" interior loading by using a crack growth function. The growth function describes basic material behaviour obtained by CA tests.

When plotting fatigue crack growth rate data of these tests in a log/log scale vs. the stress intensity factor range (see Fig. 12), all common metals exhibit the same two major characteristics:

---

* By the way, it is no question of plane strain / plane stress as supposed in ref. (11).

- the "sigmoidal" curve shape of the test data showing three different stages I, II, III
- the dependence of the test data on the stress ratio R (the mean stress) and on the relative load level S_{max}/σ_Y (relative to the yield stress).

Describing CA test data with an analytical function, one has to take these effects into account in order to reasonably "predict" at least the crack propagation of CA tests with different load ratios or load levels. Experience shows that common growth functions modelled as a power law can easily induce errors of about 200 % in cycles even for common materials and load ratios.

Starting the discussion with stage II, crack growth rates are best described by the popular Paris-function

$$f = C \cdot \Delta K^n$$

The power law obviously matches the test data of each separate stress ratio but tends to fail when the range of R-values applied broadens. On the other hand, the function proposed by Paris has its merits with regard to limit considerations, e.g. worst case analyses in nuclear engineering.

In an empirical approach, R could be introduced as a new independent variable, as done, e.g., by Walker (14)

$$f = C \cdot \{ (1-R)^{m-1} \cdot \Delta K \}^n$$

According to this function the log/log curves for tests with different R-values are all parallel. The "distance" parameter expressed in terms of R is determined by data fitting regardless of the physical meaning.

Crack closure due to plastically deformed material left in the wake of the propagating crack occurs at CA loading of any stress ratio. Assuming small scale yielding the closure condition will remain almost unchanged during most of the specimen's life. Therefore the crack opening load S_{op}, too, has to be constant for each particular CA test, but it obviously depends on the stress ratio R and also on the load level S_{max}/σ_Y. Replacing Walker's "distance" parameter by the S_{op}-function of the material one gets the growth function

$$f = C \cdot \{\Delta K_{eff}\}^n = C \cdot \{K_{max} - K_{op}\}^n = C \cdot \{\frac{1 - S_{op}/S_{max}}{1 - R} \cdot \Delta K\}^n$$

which is a proper analytical description of the test data (see Fig. 11) without relying too much on data fitting. Especially extrapolation for R-values outside the tested range is supposed to be less dangerous.

Assuming small scale yielding conditions, S_{op} should only be a function of the stress ratio and the load level, and therefore be independent of material properties other than σ_Y and of structural parameters other than the state of stress. Thus, as an engineering approach, any known S_{op}-function can be used, either measured or calculated, Fig. 10. Ananalytical function which is very close to the calculated values even in the negative R-regime has lately been suggested by Marissen et al. (17).

However it is a pressing necessity to check the growth function versus the test data (Fig. 11) and to compare each experimental crack growth curve a(N) with the respective "prediction".

As to S_{op}-measurements, a new suggestion should be mentioned. According to de Koning (18), loads measured by crack arrest after peak loads can be very similar to those of equivalent CA test, Fig. 10. Although experimentally attractive - since it needs less instrumentation - this method should be used with caution because of the following reason: While the tensile plastic zone size at the peak load application is the same as with CA loading of that magnitude, the compressive plastic zone size, hence CTOD and the resulting humps on the crack surfaces are not the same at all. By this fact, the crack opening load will differ from that of CA loading.

As to stages I and II, material data can be described employing either an empirical, e.g. the Forman-function

$$f = C \cdot \Delta K^n \cdot \frac{1}{1 - K_{max}/K_c} \qquad \text{(stage II, III)}$$

or

$$f = C \cdot \{\Delta K - \Delta K_{th}\}^n \qquad \text{(stage I, II)}$$

With his strip yield model Führing found that due to gross scale yielding in stage III a non powerlaw relationship develops between higher values of ΔK and the crack tip element CTOD range Δv_a, whereas the relationship between ΔK_{eff} and Δv_a remains a powerlaw, Fig. 13 . The Δv_a - da/dN relationship is described by a powerlaw, too. Hence, when applying the S_{op}-results of the model accounting for gross scale yielding the introduction of special empirical terms for stage III into the growth function is superfluous. So far, however, no general gross scale yielding formulation is available.

As to stage I, fatigue fracture mechanics gives the following explanation. Here, the powerlaw relationship between Δv_a and da/dN doesn't hold any longer. The threshold effect in CA test data represents not a structural mechanics but a material effect. Stage I of fatigue crack growth is very important for several industries where the stress intensities are so low that the components lives lie in transition to high cycle fatigue.

For practical purposes Newman's growth function (20)

$$f = C_1 \cdot (\Delta K_{eff})^n \cdot \frac{1 - (\Delta K_o/\Delta K_{eff})^2}{1 - (K_{max}/C_5)^2}$$

$$\Delta K_o = C_3 \cdot (1 - C_4 \cdot S_{op}/S_{max}) = U \cdot \Delta K_{th}$$

with S_{op} calculated assuming small scale yielding, seems to be appropriate to empirically describe all three stages of crack growth. However, its applicability has to be checked for other materials than aluminium where it obviously works in the R-regime studied, see Fig. 12.

CATEGORIES OF PREDICTION METHODS FOR VARIABLE-AMPLITUDE LOADING

Models for the prediction of variable-amplitude (VA) loading can be classified by the amount of computational resources they need. Three different categories are defined:

1. Large mainframe computers are necessary to compute ΔK_{eff} for each cycle employing nonlinear continuum mechanics, e.g. the finite element method or a strip yield model.
2. Minicomputers are sufficient to compute ΔK_{eff} on a cycle-by-cycle basis incorporating the most important fatigue crack growth mechanisms.
3. Only a "homecomputer" is needed to integrate crack growth rates determined by a characteristic-K approach.

Crack propagation predictions have to be less expensive than fatigue tests in order to be widely used. Although a strip yield model - when compared to the finite element method - strongly reduces the computer cost, the cost is still very high. Therefore, computations of the first category are used for the calculations of particular load sequence effects rather than for life estimation purposes. Newman, however, used this method for his contribution to the ASTM round robin analysis (20).

Prediction methods of the second category involve just a few computational steps per cycle. While CPU-times differ from those of third category models by the order of magnitude of the number of cycles to failure, CPU-time differences among the various models, i.e. older ones like those of Wheeler or Willenborg and newer ones like CORPUS (18) and LOSEQ (21), are less striking.

Both de Koning and Führing incorporated experiences made with a model of the first category into their simpler models (CORPUS and LOSEQ, respectively). Both found two major mechanisms

- the effect of a single peak load
- a limited structural memory

The single peak overload effect, as calculated by a strip yield model, is depicted in Fig. 14. It is evident that the influence of the overload on the CTOD range Δv_a is no longer prominent, when the crack tip reaches the end of the plastic zone associated with the peak load. The crack opening load S_{op} and the current tensile plastic zone ω^o approach the values of the corresponding CA loading when the current tensile plastic zone touches the primary plastic zone.

In CORPUS this effect is modelled with a simple On/Off-switch: The crack opening load S_{op} due to the peak load is only present as long as the crack tip is still inside the primary plastic zone. This assumption becomes more realistic when the peak-overload ratio is higher than the one depicted in Fig. 14. S_{op} is a function of the peak stress ratio and is evaluated according to the procedure previously discussed (see Fig. 10).

LOSEQ models the peak load mechanism more closely with the assumption

$$\Delta K_{eff} = U \cdot \Delta K \sim \sqrt{\omega^o}$$

The current plastic zone size ω^o is computed by means of the structural memory (22).

Limited structural memory is the second mechanism both models have in common, although the simulation of the actual structural behaviour differs largely. Fig. 15a schematically shows the development of tensile and compressive plastic zones with crack growth and the corresponding stress distributions on the ligament due to the given load sequence. It is depicted that structural memory can be simulated by simply inserting a new plastic zone into the place in memory that corresponds to its elastic plastic boundary at $x_i = a_i + \omega_i$ and cancelling the zones with a smaller x. This scheme is also used to calculate the zone's actual size (21).

CORPUS models the behaviour of humps on the crack surface (Fig. 15b). Each hump originates from a peak load. The associated crack opening load is taken from the above mentioned S_{op}-function (Fig. 10), and changes according to the same function in case the hump is submitted to plastic compression by contact. The highest of all the hump's individual crack opening loads is the overall crack opening load of the current loading cycle.

Both models were developed to work with flight-spectra of aircraft components. They have been successfully applied for various tasks in life estimation. It should be stated, that the conception of both models has weak and strong points. If load interaction takes place while the crack tip is still inside the primary plastic zone, LOSEQ is supposed to give a better life estimation, whereas CORPUS is better suited to predict the effect of few high compressive underloads, e.g. ground-to-air-cycles of flight-spectra, affecting the humps and not only the ligament stress distribution.

In a model of the third category, Schijve (23) - in order to enable an integration of crack growth rates - assumes that the crack opening load is almost constant for the whole - stationary - VA loading sequence. Furtheron he assumes that the S_{op}-value can be computed from the S_{op}-function (Fig. 10) using load spectrum maxima and minima. After these simplifying steps the spectrum-dependent crack growth rates can be determined and easily integrated.

All three models besides others, are being checked on flight-spectra, such as F-27 and FALSTAFF, in the GARTEUR round-robin activity on fatigue crack propagation prediction (24).

Concluding Remarks

The last section of the paper contains fatigue crack growth aspects with special emphasis on aircraft application, but nowadays other industries commence to apply the mentioned more sophisticated prediction techniques, too. Besides the here presented "fatigue fracture mechanics" approaches which are essentially based on the local elasto-plastic structural behaviour, other approaches exist which attack the problem by applying common linear accumulation of CA data. Furtheron, in these models the load interaction effect of variable amplitude loading on life is described by modified values of the damage sum.

In literature, many contributions can be found where such approaches succeed in giving valuable life estimations. However, from nature they can be only successful in a very close range of application. Their merits lie for instance in the field of load spectra being almost of CA type where only the load level is slightly altered.

General purpose computer programs for fatigue life estimation can only be written when based on the knowledge of local fracture phenomena. It is acknowledged, however, that not all details have been solved yet and some of the most pressing problems of industry (see the keywords in Fig. 1) still wait for their solution.

List of references

1. Bartholome,G., Steinbuch ,R., Wellein,R., Proceedings 7th MPA Seminar,(Stuttgart, F.R.G., 1976)
2. Führing,H., Seeger,T., Proceedings 2nd International Conference on Mechanical Behaviour of Materials,(Boston, 1976).
3. Führing,H., Seeger,T., Engng.Frac.Mech., (1979) 99.
4. Rice,J.R., ASTM STP 415, (1967), 247.
5. Seeger,T., "Ein Beitrag zur Berechnung von statisch und zyklisch belasteten Rißscheiben nach dem Dugdale-Barenblatt Modell" (Institut für Statik und Stahlbau, Darmstadt, F.R.G., 1973).
6. Führing,H. and Seeger,T., J.Fracture, (1977) 728.
7. Weidmann,G.W. and Döll,W., J.Fracture, (1978) R189.
8. Kunz,L., Knešl,Z., Lukas,P., Fatigue Engng.Mat.Struc., (1979) 279.
9. Budiansky,B., Hutchinson,J.W., J.appl.Mech., (1978) 267.
10. Jones,J.W., Macha,D.E., Corbly,D.M., J.Fracture, (1978) R25.
11. Ohta,A., Kosuge,M., Sasaki,E., J.Fracture, (1979) R53.
12. Sharpe,W.N.Jr. and Grandt,A.F.Jr., ASTM STP 590, (1976) 302.
13. Führing,H., J.Fracture, (1976) 917.
14. Walker,K., ASTM STP 462, (1971) 1.
15. Elber,W., ASTM STP 486, (1971) 230.
16. Führing,H., "Berechnung von elastisch-plastischen Beanspruchungsverläufen in Dugdale-Rißscheiben mit Rißuferkontakt auf der Grundlage nichtlinearer Schwingbruchmechanik", (Institut für Statik und Stahlbau THD, Darmstadt, F.R.G., (1977).
17. Marissen,R., Trautmann,K.H., Nowack,H., to be published in Engng.Frac.Mech., (1984).
18. de Koning,A.U., ASTM STP 743, (1981) 63.

19. Schijve,J., Engng.Frac.Mech., (1981) 461.
20. Newman,J.C.Jr., ASTM STP 748, (1981) 53.
21. Führing,H., "Modell zur nichtlinearen Rißfortschrittsvorhersage unter Berücksichtigung von Lastreihenfolge-Einflüssen (LOSEQ)", (Fraunhofer-Institut für Betriebsfestigkeit LBF, Darmstadt, F.R.G., 1982).
22. Führing,H., ASTM STP 677, (1979) 144.
23. Schijve,J., ASTM STP 700, (1980) 3.
24. van der Linden,H.H., "A Check of Crack Propagation Prediction Models against Test Results Generated under Transport Aircraft Flight Simulation Loading", to be published, (National Aerospace Laboratory NLR, Amsterdam, The Netherlands, 1984)

	Power Generation / Processing			Heavy Industry		Transport Vehicles		
	Nuclear Power Plants	Chemical Plants	Conventional Power Plants	Steel Production	Mining	Off-Shore, Ships	Trains	Trucks, Cars	Airplanes, Space
Components	pipes, vessels, valves			shafts, rolls	framework, cranes, derricks	ship hulls, nodes	rails, wheels (bridges)	chassis framework lugs	fuselage, wings, landing gear
		oil-pipelines							
Type of Loading	internal pressure, high temperatures			concentrated heavy loads		(waves)	load fluctuations		(gust loads)
	(radiation)	(aggressive environment)							
Materials	high-alloy ferritic and austenitic steels (nickel-base alloys)			low alloy ferritic steels	structural steels		structural steels light metals (reinforced plastics)		
Interests in Fract. Mech.	quality assurance failure analysis safety concepts inspection			failure analysis life estimation			quality control failure analysis life estimation surveillance		
F. M. Problem Areas	leak-before-burst part-through cracks creep-fatigue	fatigue		laminar tearing	thick-wall problems welds	load spectra	thin-wall problems prediction methods for VA loading		

Fig. 1 Overview on fracture mechanics application in industry

Fig. 2 Current employment of fracture mechanics in industry

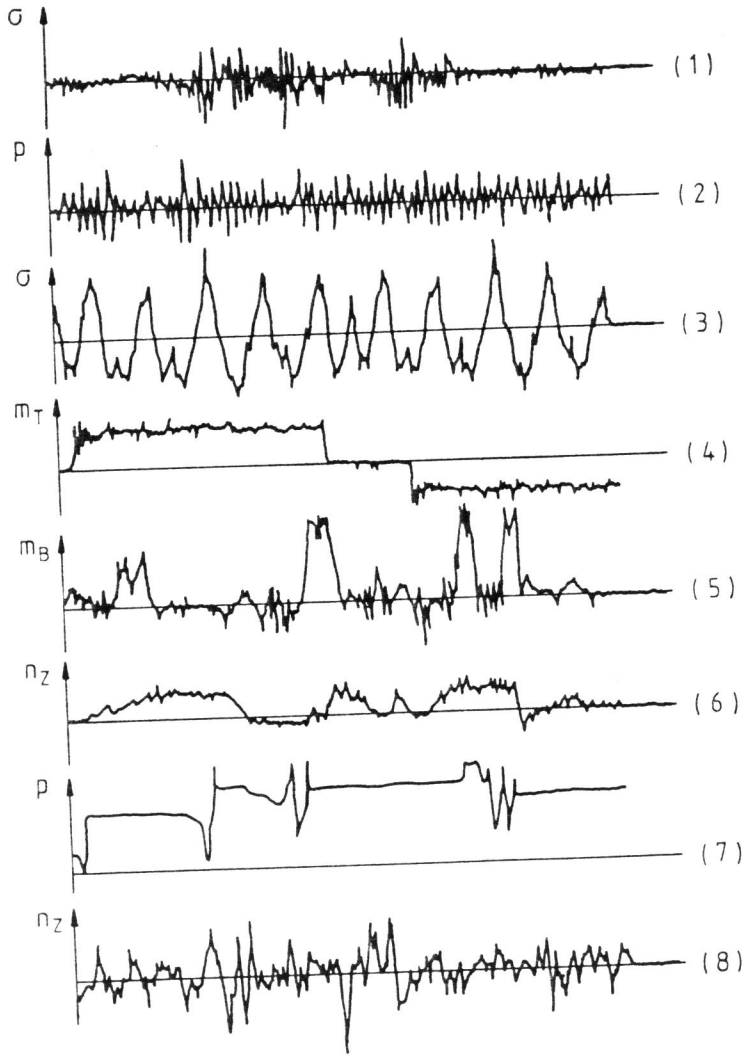

Fig. 3 Typical measurements of loading sequences (by LBF)

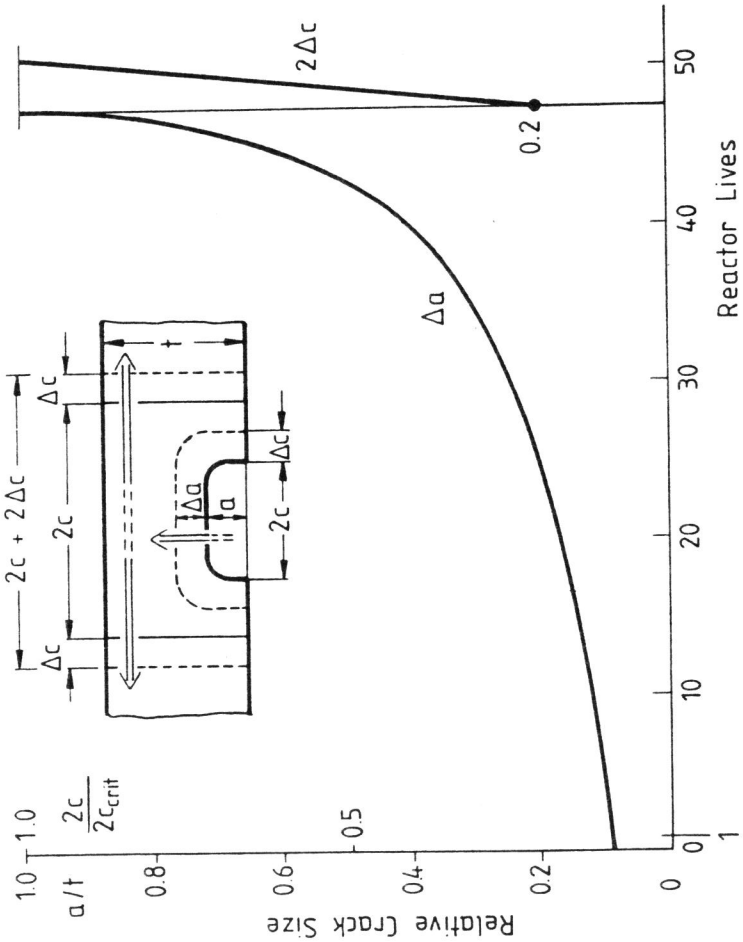

Fig. 4 Growth of a circumferential part-through and through crack in the wall of a primary coolant pipe, KWU [1]

Fig. 5 Rest-life estimation for the postulated axial cracks in the primary sodium piping system (SNR-300) when detected by leakage

(a) Compact Fracture Mechanics Specimen (b) Load-Displacement Diagram (c) Magnified Crack Tip Configuration

Fig. 6 Crack tip deformations illustrating the damage stages of a monotonically loaded CT specimen

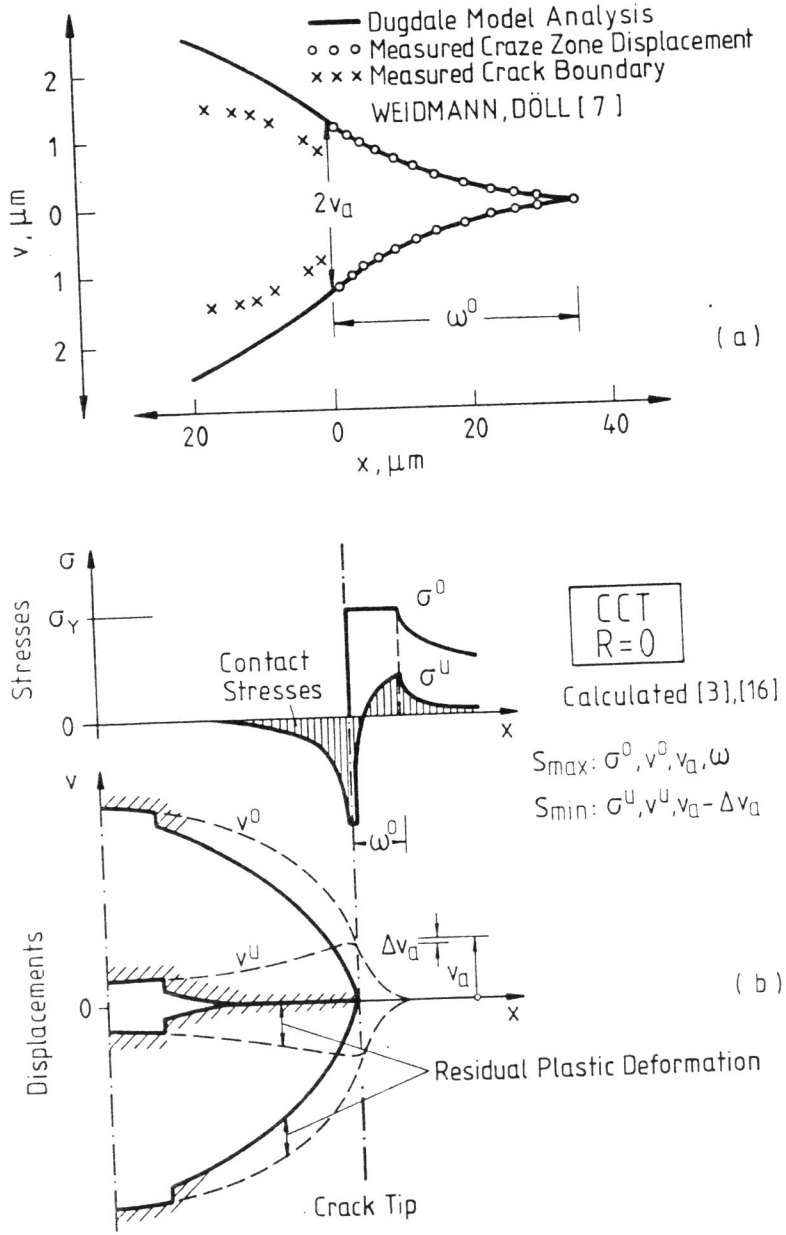

Fig. 7 Correspondence of measurement (a) and extended Dugdale model analysis (b) with regard to the crack displacements

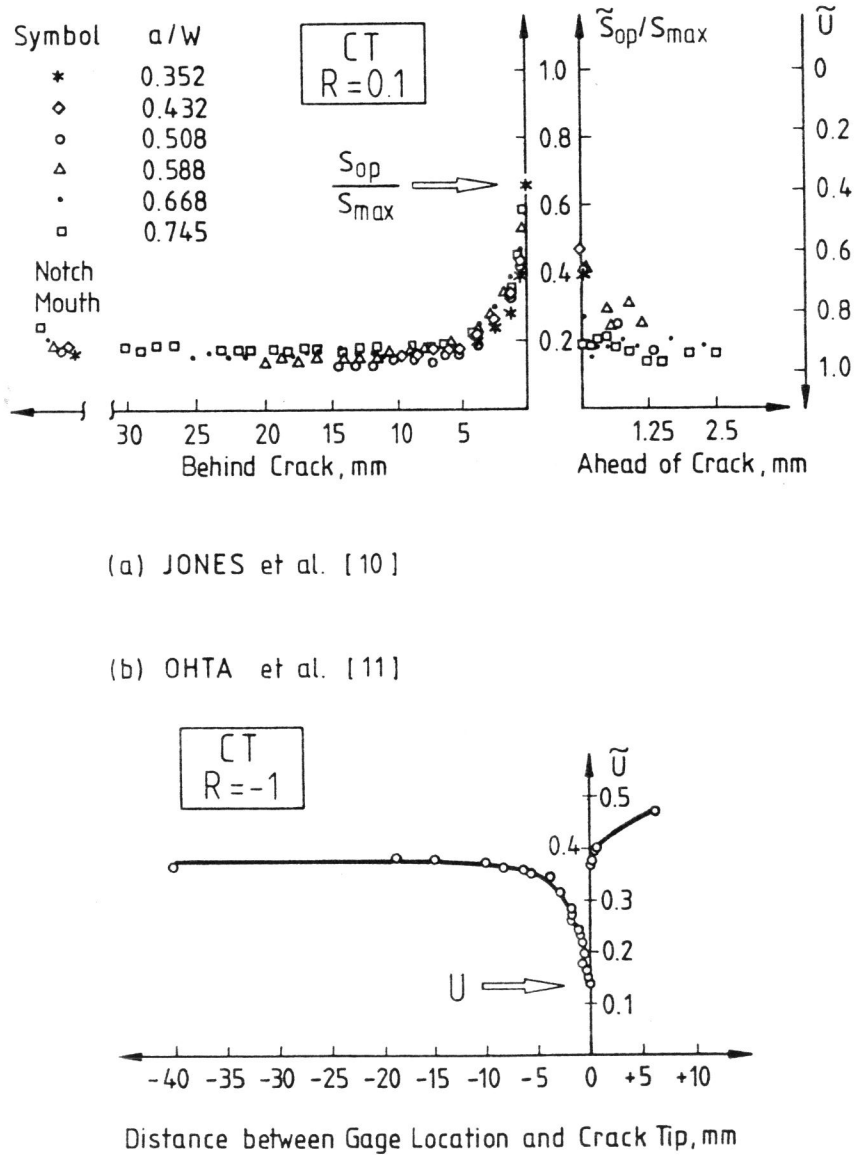

Fig. 8 Dependance of observed crack opening values on the "gage" location and real S_{op}-values indicated by arrows.

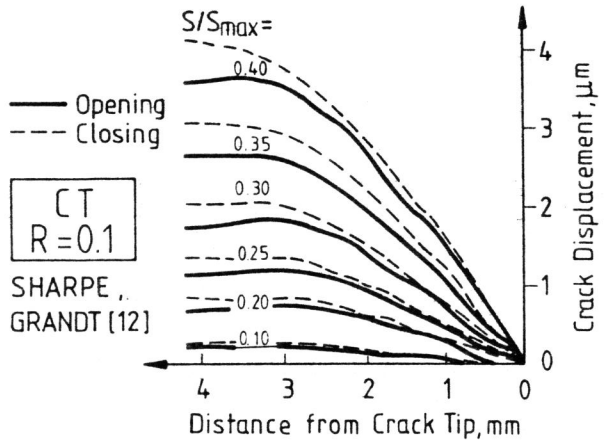

Fig. 9 Measurement of the crack profile during unloading and loading showing partial crack closure and opening

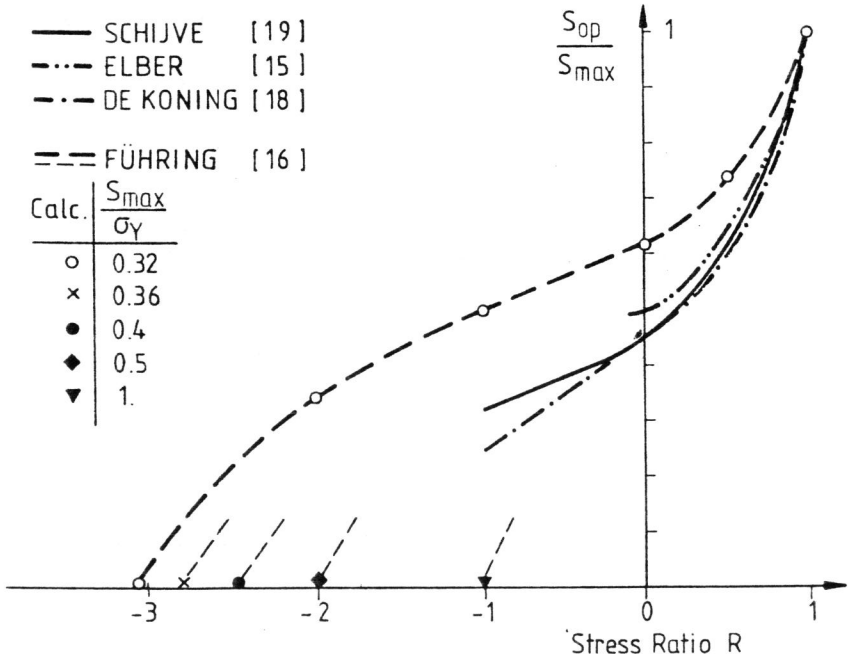

Fig. 10 Measured and calculated crack opening loads as a function of stress ratio for CA and peak load tests.

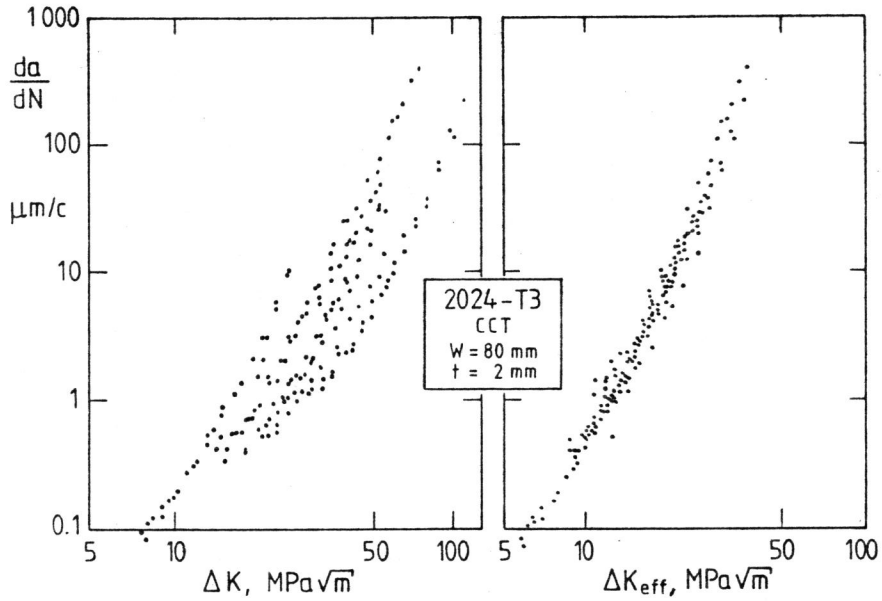

Fig. 11 Semi-empirical Growth Function, Stage II, SCHIJVE [19]

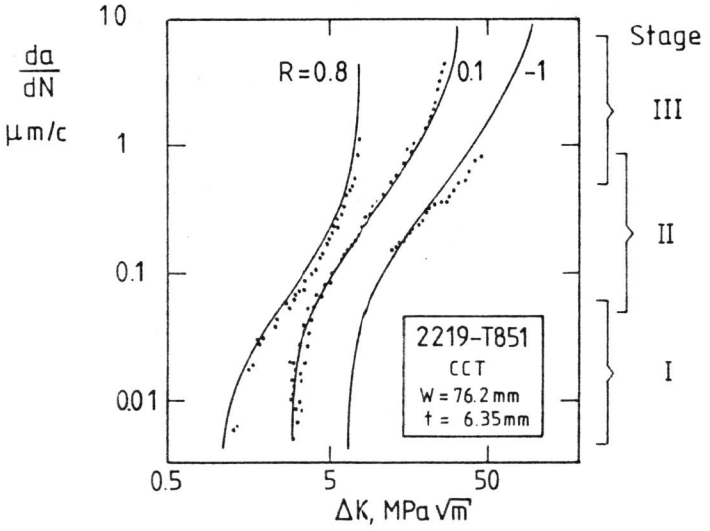

Fig. 12 Semi-empirical Growth Function, NEWMAN [20]

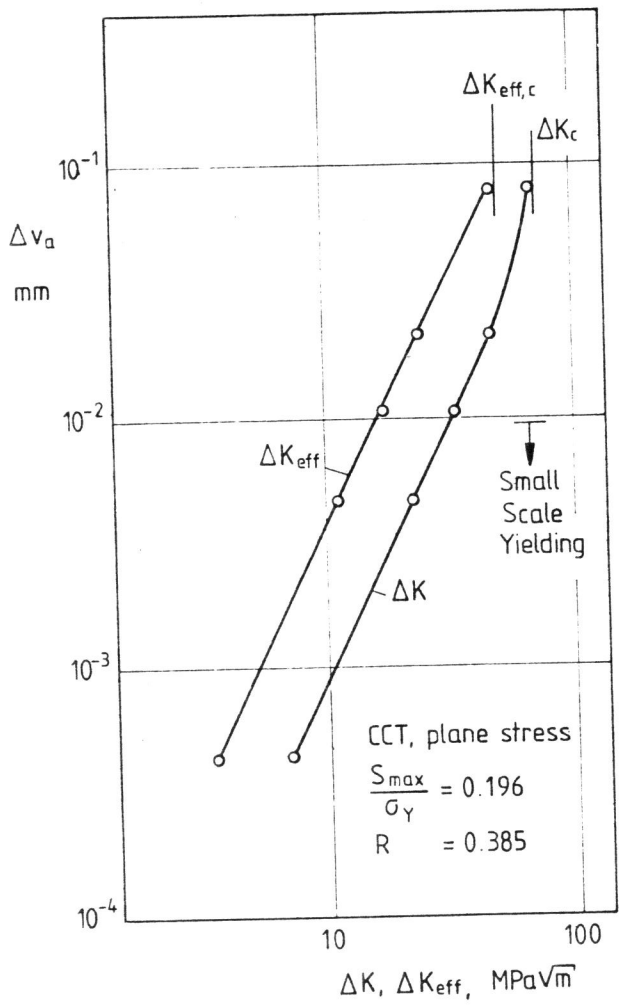

Fig. 13 Calculated Fatigue Crack Growth in Stage II, III - the Effect of Gross Scale Yielding, FÜHRING [16]

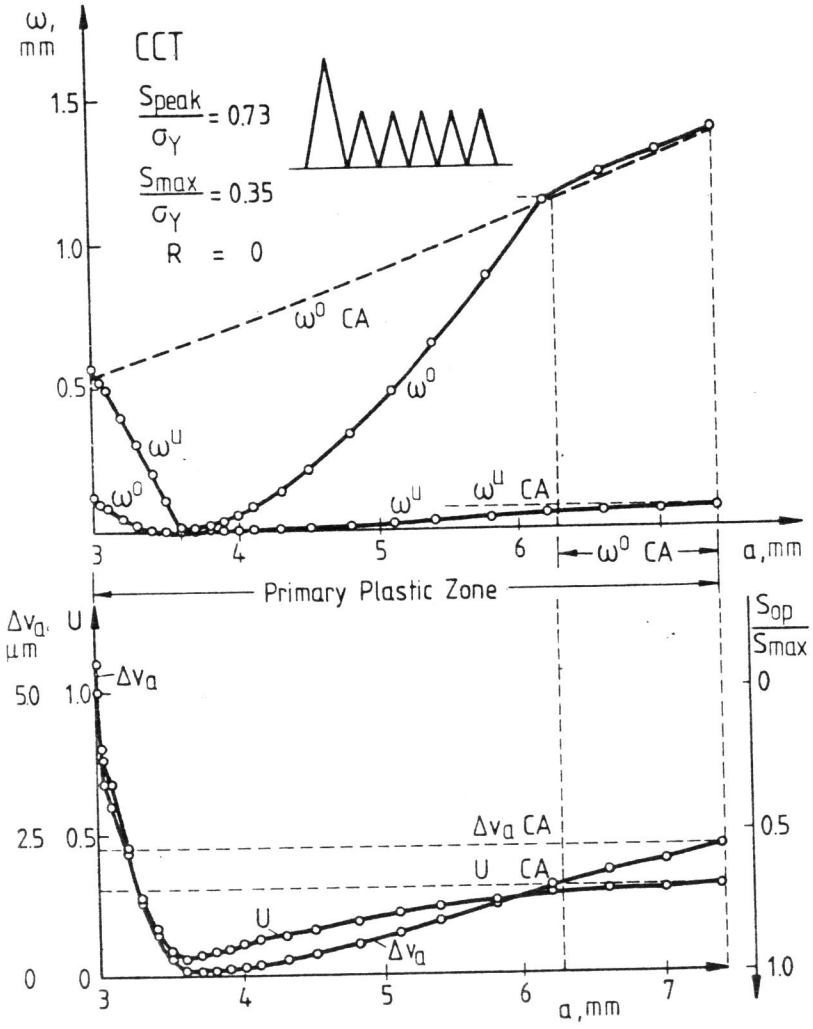

Fig. 14 The effect of a peak load. Calculated by a strip yield model, FÜHRING [16]

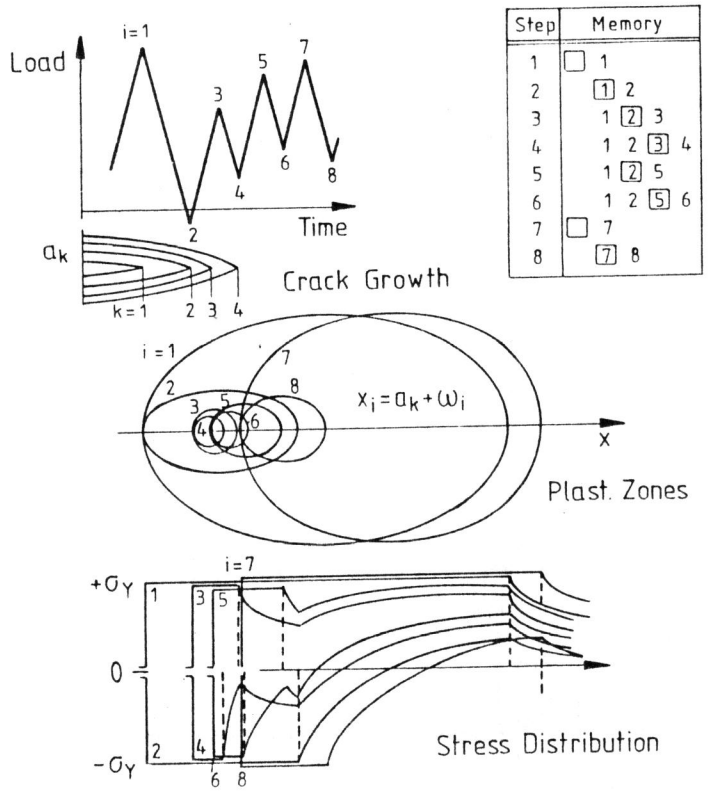

(a) LOSEQ [21]

(b) CORPUS [18]

Fig. 15 Two models of structural memory